Accepted Manuscript

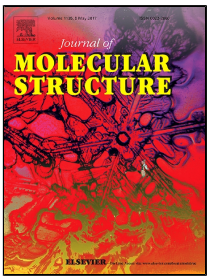

Synthesis, structural, catecholase, tyrosinase and DFT studies of Pyrazoloquinoxaline derivatives

Zohra Bouanane, Mahmoud Bounekhel, Meriem Elkolli, Farid Abrigach, Mohamed Khoutoul, Rabab Bouyala, Rachid Touzani, Abdelkader Hellal

PII:	S0022-2860(17)30323-X
DOI:	10.1016/j.molstruc.2017.03.052
Reference:	MOLSTR 23548
To appear in:	*Journal of Molecular Structure*
Received Date:	25 January 2017
Revised Date:	11 March 2017
Accepted Date:	11 March 2017

Please cite this article as: Zohra Bouanane, Mahmoud Bounekhel, Meriem Elkolli, Farid Abrigach, Mohamed Khoutoul, Rabab Bouyala, Rachid Touzani, Abdelkader Hellal, Synthesis, structural, catecholase, tyrosinase and DFT studies of Pyrazoloquinoxaline derivatives, *Journal of Molecular Structure* (2017), doi: 10.1016/j.molstruc.2017.03.052

Graphical Abstract

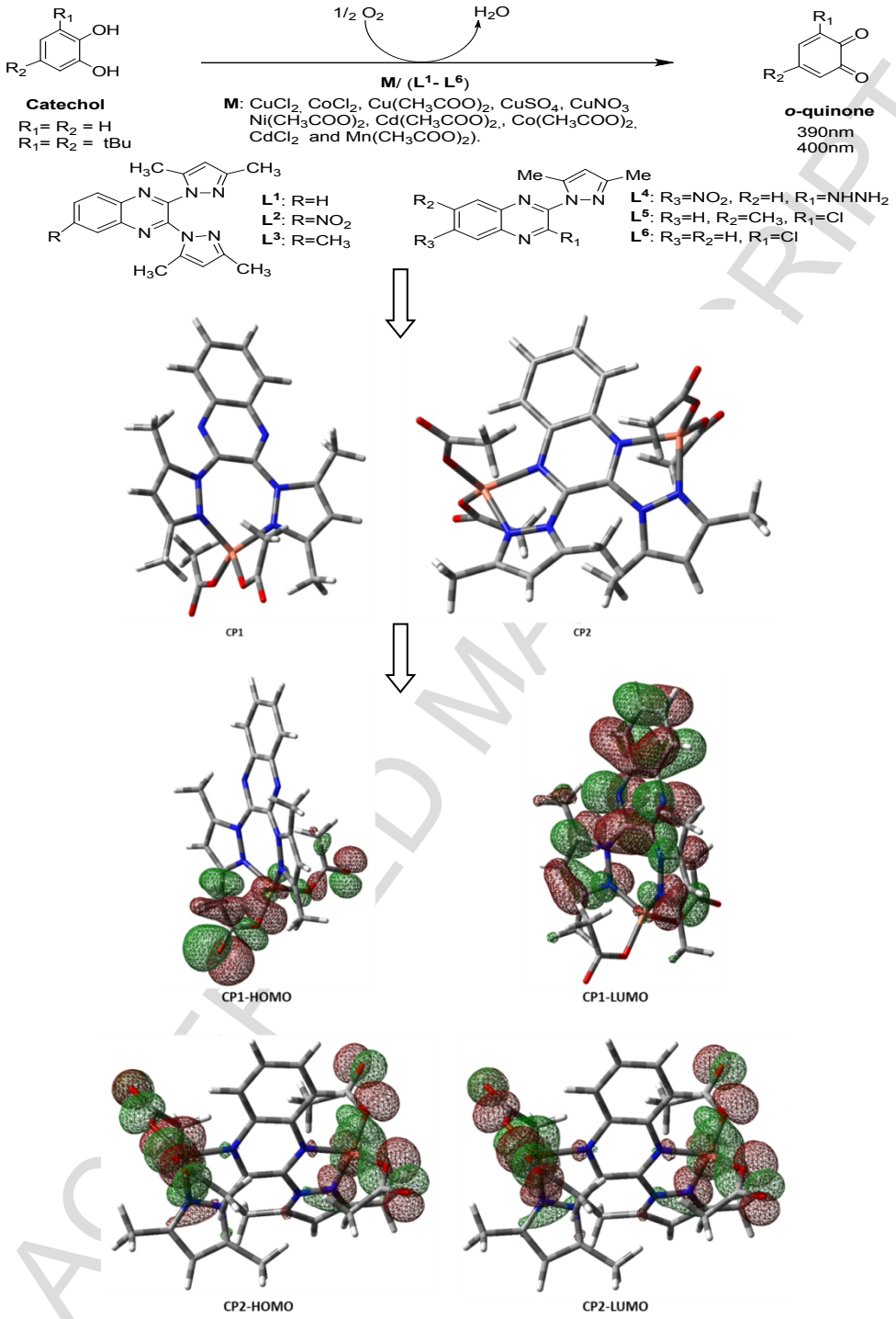

Highlights

- Syntheses and characterization of pyrazoloquinoxaline
- Catecholase and tyrozinaze oxidation reaction
- All prepared *in-situ* complexes catalyze the oxidation reaction of catechol
- Oxidation reaction rate depends on four parameters.
- The highest rate activity is given by L^1 $[Cu(CH_3COO)_2]$ V= 33.48 $\mu molL^{-1}min^{-1}$
- Use of DFT for electronic structure elucidations.

Synthesis, structural, catecholase, tyrosinase and DFT studies of Pyrazoloquinoxaline derivatives

Zohra Bouanane[a,*], Mahmoud Bounekhel[a], Meriem Elkolli[a], Farid Abrigach[b], Mohamed Khoutoul[c], Rabab Bouyala[c], RachidTouzani[b,c] , Abdelkader Hellal[d]

[a]*Laboratoire des matériaux polymériques multiphasiques « LMPMP », Département de génie des procédés, Faculté de technologie, Université Ferhat Abbas, Sétif-19000, Algérie.*
[b]*Laboratoire de Chimie Appliquée et Environnement, Département de Chimie, Faculté des Sciences, Université Mohamed Premier, BP 524, 60 000 Oujda, Maroc.*
[c]*Faculté Pluridisciplinaire de Nador, Université Mohamed Premier, BP300, Selouane 62700, Nador, Maroc.*
[d]*Laboratoire d'Electrochimie des Matériaux Moléculaires et des Complexes « LEMMC », Département de génie des procédés, Faculté de technologie, Université Ferhat Abbas, Sétif-19000, Algérie.*
Corresponding authors: E-mail: syntorg@hotmail.fr (Z. Bouanane) *or* haekpharm @yahoo.fr (A. Hellal).

Abstract

Six functional multidentate ligands: 2,3-bis(3,5-dimethyl-1H-pyrazol-1-yl) quinoxaline, **L^1**, 2,3-bis(3,5-dimethyl-1H-pyrazol-1-yl)-6-nitroquinoxaline, **L^2**, 2,3-bis(3,5-dimethyl-1H-pyrazol-1-yl)-6-methylquinoxaline, **L**^{3}, 2-(3,5-dimethyl-1H-pyrazol-1-yl)-3-hydrazinyl-6-nitroquinoxaline **L^4**, 2-chloro-3-(3,5-dimethyl-1H-pyrazol-1-yl)-6-methylquinoxaline, **L^5**, 2-chloro-3-(3,5-dimethyl-1H-pyrazol-1-yl) quinoxaline, **L**^{6}, and a new copper (II) complex, were prepared and evaluated for their catecholase activities at aerobic conditions. We found that, the reaction rate depends on: The nature of the substituents in the quinoxaline ring, counter anion, metal, concentration of ligand and the used solvent. The complex obtained *in-situ* from reaction of one equivalent of ligand **L^1** and two equivalents of $Cu(CH_3COO)_2$ in methanol showed the highest oxidation rate activity (V= 33.48 $\mu mol.L^{-1}.min^{-1}$). In addition, geometry optimizations of the complexes in order to get better insight into the geometry and the electronic structure and chemical reactivity were carried out by means of DFT calculations.

Keywords: Multidentate ligands**,** Pyrazoloquinoxaline, Copper, Tyrosinase, Catecholase, DFT, HOMO, LUMO.

1. Introduction

Copper plays an important role in biological systems, where it is mainly bound in metalloenzymes. These enzymes are involved in many processes such us hydroxylation, oxygen transport, electron transfer, and catalytic oxidation [1-8]. Recently, many works have been devoted to the copper complexes based on pyrazole ligands to mimic the function of catecholase [9-14]. In fact, the imidazole ring of histidine residues is one of the most common ligands at the active sites of metalloproteins, which guided us to use pyrazole which have a similar structure of imidazole to mimic the function of catecholase active site. The pyrazole based ligands present important results in terms of oxidation rate, which sometimes attains 28.99 $\mu mol.L^{-1}.min^{-1}$ [15].

In this study, six ligands **L^1-L^6**, were reported and examined for their catecholase activities at ambient conditions. The metallic complexes formed *in-situ* from **L^1-L^6** and different metal salts (MX_2: $CuCl_2$, $Cu(CH_3COO)_2$, $CuSO_4$, $Cu(NO_3)_2$, $Ni(CH_3COO)_2$, $Cd(CH_3COO)_2$, $CdCl_2$, $Co(CH_3COO)_2$, $CoCl_2$ and $Mn(CH_3COO)_2$ show significant catalytic influence pathway on the

oxidation of catechol and 3,5-DTBC to the corresponding *o*-quinones via formation of dinuclear species. To more understand the parameters influencing the catalytic activity of the studied complexes and to understand the key properties of solvents which have a controlling role in the catecholase activity, the effect of ligand concentration, the nature of substrate, and the effect of the solvent are studied. The reaction follows Michaelis–Menten [16], enzymatic reaction kinetics to determinate the kinetic parameters.

In the present investigation, common DFT-based reactivity descriptors are consequently included for their importance during the actual study. The DFT cover systems between a few tens up to a few hundreds of atoms. It is often of wide-ranging applicability and reasonably accurate in many cases. The 1998 noble prize in chemistry recognized the convergence of traditional quantum chemical methodology and DFT [17]. In fact, DFT has enjoyed an enormous popularity in this field over the past two decades and has found many users that range from hardcore theoretical chemists to experimentalists who wish to employ DFT along side with their experimental studies. Parallel with the impressive development of computational hardware the quantum chemical software that is required to perform DFT calculations has progressed to a state where calculations can be performed with high efficiency and in a user friendly manner [18-21].

In the present study, the structure and the ground state energy of the molecules under investigation have been analyzed employing gas phase using DFT/B3LYP (C, H, N and O)/LanL2DZ (Cu) level calculations. The optimized geometry and their properties such as equilibrium energy, frontier orbital energy gap, have also been used to understand the activity of these compounds. Density functional theory has been found to be successful in providing insights into the chemical reactivity and stability, the analysis of the frontier molecular orbitals is a crucial way to obtain information on reactivity of molecules and to study electron excitation from the highest occupied molecular orbital (HOMO) to the lowest unoccupied molecular orbital (LUMO).

2. Experimental section

2.1. Instruments

The ^{1}H NMR and ^{13}C NMR spectra were recorded on a Bruker 300 spectrometer. Chemical shifts are listed in ppm and are reported relatively to TMS. The Infra-red spectra were taken using KBr discs on Mattson Genisis FTIR. The mass spectra have been obtained on a SHIMADZU Axima-CFR MALDI-TOF. **L^1** has spectral data in accordance with the literature data [22]. A new complex **CP_1** was synthesized and characterized by means of IR and UV by Z. Bouanane and co-workers [23].

2.2. Synthesis

2.2.1. General method for synthesis of ligands L^2 and L^3:

Acetylacetone (15mL, 25 mmol) was added to a suspension of 2,3-hydrazinoquinoxaline **2b-c** (3 mmol, 6,88g) in 250 ml of ethanol . The mixture was stirred under reflux for 4 hours, the solvent was removed and the compounds were purified by column chromatography with hexane/ethyl acetate(7/3:v/v).

2,3-bis(3,5-dimethyl-1H-pyrazol-1-yl)-6-nitro quinoxalines, L^2. Yield: 83%. FTIR (KBr, cm^{-1}): 2978, 2892, 1599, 1393.^{1}H NMR (300MHz, $CDCl_3$, δ, ppm): 9.00 (s, H_5, 1H); 8.56 (dd,

H_7,1H); 8.24 (dd, H_8,1H); 6.01(s, H-pz, 2H); 2.42(s, pz-CH_3, 6H); 2.15 (s, pz-CH_3, 6H). ^{13}C NMR (75MHz, $CDCl_3$, δ, ppm) : 151.4-138.5 (C); 130.1-124.0(CH); 108.4-108.1(CH pz); 13.5 (CH_3); 12.0 (CH_3); MALDI-TOF (ES) m/z (%) = 364.17 (80) ; 363.14 (70) ; 362.21 (100).

2,3-bis(3,5-dimethyl-1H-pyrazol-1-yl)-6-methyl quinoxalines, L³. Yield: 85%. FTIR (KBr, cm^{-1}):2940, 2850, 1595, 1384. ^{1}H NMR (300MHz, DMSO, δ , ppm) :8.58 (dd, H_8, 1H); 8.25 (s, H_5,1H); 8.15 (dd, H_7,1H); 6.09(s, H-pz, 2H); 2.53 (Aromatique-CH_3); 2.42(s, pz-CH_3, 6H); 2.15 (s, pz-CH_3, 6H). ^{13}C NMR (75MHz, DMSO, δ, ppm): 149.9-138.0 (C); 130.2-124.3(CH); 108.0-107.8 (CH pz); 20.6 (Aromatique-CH_3); 13.2 (CH_3); 11.6 (CH_3); MALDI-TOF (ES) m/z (%) = 334.24 (35) ; 333.24(100) ; 332.22 (25) ; 331.23 (90).

2.2.2.General method for synthesis of ligands, L⁴-L⁶:

Acetylacetone (0.11mL, 1.1mmol) was added to a suspension of 2-chloro-3-hydrazinoquinoxaline **2b-c** (0.27 g, 1 mmol) in 50 ml of ethanol . The mixture was stirred under reflux for 18 hours, the solvent was removed and the compounds were purified by column chromatography with hexane/ethyl acetate(7/3:v/v).

2-(3,5-dimethyl-1H-pyrazol-1-yl)-3-hydrazinyl-6-nitroquinoxaline, L⁴. Yield: 78%.FTIR (KBr, cm^{-1}): 3448, 3281, 1629, 1552, 1487, 817. ^{1}H NMR (300MHz, DMSO, δ , ppm) :8.91 (d, H_8, 1H); 8.50 (dd, H_6,1H); 8.02 (d, H_5,1H); 6.18(s, H-pz, 2H); 4.24 (hydrazine-NHNH_2); 2.43(s, pz-CH_3, 3H); 2.36 (s, pz-CH_3, 3H). ^{13}C NMR (75MHz, DMSO, δ, ppm) : 149.9-138.0 (C); 130.2-124.3(CH); 108.0-107.8 (CH pz); 20.6 (Aromatique-CH_3); 13.2 (CH_3); 11.6 (CH_3); MALDI-TOF (ES) m/z (%) = 334.24 (35) ; 333.24(100) ; 332.22 (25) ; 331.23 (90).

3-chloro-2-(3,5-dimethyl-1H-pyrazol-1-yl)-6-methylquinoxaline, L⁵ , Yield: 92%.FTIR (KBr, cm^{-1}): 2766, 1630, 802. ^{1}H NMR (300MHz, DMSO, δ , ppm) :8.17-8.01 (m, H_8, H_5, 2H); 7.87-7.78 (m, H_6, H_7,2H); 8.15 (dd, H_7,1H); 6.08(s, H-pz, 1H); 2.34 (Aromatique-CH_3); 2.34(s, pz-CH_3, 3H); 2.32 (s, pz-CH_3, 3H). ^{13}C NMR (75MHz, DMSO, δ, ppm) : 149.9-138.0 (C); 130.2-124.3(CH); 108.0-107.8 (CH pz); 20.6 (Aromatique-CH_3); 13.2 (CH_3); 11.6 (CH_3).

*2-chloro-3-(3,5-dimethyl-1H-pyrazol-1-yl)quinoxaline, L⁶,*Yield: 89%.FTIR (KBr, cm^{-1}): 3039, 2915, 1635, 770. ^{1}H NMR (300MHz, DMSO, δ , ppm) :7.98 (d, H_5, 1H); 8.25 (s, H_8,1H); 8.15 (dd, H,1H); 6.10(s, H-pz, 2H); 2.60 (Aromatique-CH_3); 2.35(s, pz-CH_3, 3H); 2.31 (s, pz-CH_3, 3H). ^{13}C NMR (75MHz, DMSO, δ, ppm) : 150.9-139.8 (C); 142.0-127.7(CH); 107.5 (CH pz); 21.9(Aromatique-CH_3); 13.7 (CH_3); 11.7 (CH_3).

2.3.Catecholase Activity Measurements

Kinetic measurements were made spectrophotometrically on UV-Visible spectrophotometer (In the COSTE: Centre de l'Oriental des Sciences et Technologies de l'Eau), following the appearance of *o*-quinone over time at 25°C (390 nm absorbance maximum, ε = 1600 $M^{-1}.cm^{-1}$ in methanol,ε = 1900 $M^{-1}.cm^{-1}$ in THF and ε = 1600 $M^{-1}.cm^{-1}$ in acetonitrile). The metal complex solution (prepared *in-situ*: 1 mL of a 2.10^{-3}M ligand and metal salt solution) and a solution of catechol (2 mL of a 10^{-1}M solution) were mixed in the spectrophotometric cell.

2.4 Computational details

All calculations were performed using the GAUSSIAN 09 program package [24] with the aid of the GaussView visualization program [25]. The ground state geometries of **CP_1** and **CP_2**

were fully optimized using the hybrid B3LYP functional methods [26-27] in combination with the 6-31G (d) basis set for C, H, N and O, while for Cu, the LanL2DZ basis set with effective core potential were used [28].

3. Results and discussion

3.1. Synthesis

The pyrazolyl derivatives, **L^1-L^6**, were prepared respectively by a three-step process involving the synthesis of chloroquinoxaline **1a-c** [29] and hydrazinoquinoxaline derivatives **2a-e** [30]. Followed by a condensation of 2,4-pentanedione with hydrazinoquinoxaline derivatives in anhydrous solvents (Scheme 1). All compounds were characterized by means of IR, ^{1}H-NMR, ^{13}C-NMR and mass spectrometry techniques.

The new ligands **L^3** and **L^4** were obtained with good yield (85-90%). The absence of bands between 3200 and 3400 cm^{-1} in IR spectra, demonstrated that the pyrazole compounds is formed. The proton NMR spectra of the pyrazolic ligands revealed signals at 6.09-5.96 ppm corresponding to the pyrazolic protons (-CH-pz). The influence of different R groups is visible on the chemical shift in ^{1}H NMR of the aromatic protons of quinoxaline.

The Complex **CP_1**was characterized by MALDI-TOF mass technique. The value M (m/z) = 517.16 on the Fig.1 corresponding to the mass of CP1 plus a molecule of water.

3.2. Catalytic activity studies

The progress of the catechol oxidation reaction is conveniently followed monitoring the strong absorbance peak of *o*-quinone in the UV/Vis spectrophotometer (Scheme 2). The metal complex (prepared *in situ* from metal salt and the ligand) [31] and a solution of catechol were added together in the spectrophotometric cell at 25°C. Formation of *o*-quinone was monitored by the increase in absorbance at 390 and 400 nm as a function of time. In all cases, catecholase activity was noted.

3.2.1. Effect of ligand concentration on the catecholase activity

To understand the effect of ligand concentration to form the catalyst of the oxidation reaction of catechol to *o*-quinone, we realized this reaction using different concentration of ligand and metal ion (L/M: 1/1; 2/1; 1/2), after monitoring the absorbance of *o*-quinone for each proportion (Fig. 2). The results obtained showed a change in absorbance at 390 nm as a function of time during the first hour of the reaction, which can explains the combinations used as catalyst, catalyze the reaction well studied, and it is clear that there to differences in the absorbance values for each combination, according to these values, the combination formed by 2 mole of metal and one mole ligand appears the best catalytic condition for this reaction. After comparison of results showed in Tables 1, it appears that there is a difference in obtaining values of the oxidation rate; this difference may be related to the effect of the ligand concentration, which can be explained by the nature of coordination environment. Based on the information which confirms that the active site of the enzyme catecholase contains two Cu (II) ions [32], so, our complexes must contain two cupric ions Cu(II) to do its catalytic function, so we can propose that one molecule of ligand can participate in coordination of two ions Cu(II).

3.2.2. Effect of the nature of ligand

The nature of the ligand particularly the electronic effect of substituent group could modify coordination. The presence of donor and acceptor substituents in **L^2** and **L^3**, explain that the complex with these ligands has the lowest value of catalytic activity. If we examine well the structures of all ligands **L^1–L^6** and the obtained results (Fig.3) of catecholase activities of this variety of complexes, we notice that the substituents on the pyrazole rings have a strong effect on the oxidation reaction. As can be seen from Table 1, all of the complexes catalyze the oxidation reaction of catechol to *o*-quinone with the rate varying from a higher one of 33.48 µmol.L^{-1}.min^{-1} for the **L^1[Cu($CH_3COO)_2$]** complex to a weaker rate of 8.36 µmol.L^{-1}.min^{-1} for **L^1[Cu($CH_3COO)_2$]** complex**.** The catalytic activities depend strongly on both the form of the ligand chains and the concentration of the metallic salt. The order of reactivity for the oxidation of catechol by **Cu ($CH_3COO)_2$** complexes is **L^1>L^2>L^3> L^4>L^5>L^6**.

3.2.3. Effect of the nature of the metal and the anion

The oxidation rate depends strongly on both the ligand and the type of metals. The nature of the metals affects the geometry of the complex. This factor can contribute to the explanation of the oxidation rate dependence in the oxidization of catechol in *o*-quinone.

In the case of Cl^- and NO_3^- anions (Fig. 4), the complex of the ligand **L^1** with metals **Co(II)** and **Cu(II)** give an oxidation rate between 1.02 and 1.10 µmol.L^{-1}.min^{-1} which is higher than the complexes with ligand containing nitro **L^2** and methyl **L^3** (Table 2),.We notice that most ligands have low absorbance with all the anions except the case of the metals salt of Cu(II), Co (II) and Mn(II), the oxidation rates vary from the highest value of 33.48 µmol.L^{-1}.min^{-1} for **L^1[Cu($CH_3COO)_2$]** to the weaker value of 0.03 µmol.L^{-1}.min^{-1} for**L^3, L^4**and **L^6[Cd($CH_3COO)_2$]**. On other hand, the effect of the nature of the counter anion on the catalytic activity has been noted (Table 2), this allowed us to observe that the counter anion participates in the coordination environment and its nature influences well the catalytic activity. The anions that are weakly attached with metal ion, the substrate finds no difficulty to coordinate with the metal because it can easily replace the weakly linked anions as in the case of acetate, while the anions that bind strongly to the metal cannot be easily moved by the substrate, thereby reducing the catalytic ability.

3.2.4. Effect of substrate

A study by the catecholase activity was performed using 3,5-di-tert-butyl catechol (3,5-DTBC). The absorbance was continually monitored at λ=400 nm, in the presence of combinations **L^1-L^6/ Cu($CH_3COO)_2$** (**1L/2M**) in methanol, the obtained results are in Fig.5. Lowest value of catalytic activity was found. It appears to be much more difficult to oxidize 3,5-DTBC, owing to the presence of bulky tertiary butyl substituents. The *in situ* complexes catalyze the oxidation reaction of 3,5-DTBC to 3,5-DTBQ with the rate varying from a high of 20.56 µmol. L^{-1}.min^{-1} for the **L^1[Cu($CH_3COO)_2$]** complex, 18.75 µmol L^{-1} min^{-1} for the **L^2[Cu($CH_3COO)_2$]** complex, 15.96 µmol.L^{-1}.min^{-1} for **L^3[Cu($CH_3COO)_2$]** complex, 12.77µmol.L^{-1}.min^{-1} for the **L^5[Cu($CH_3COO)_2$]** complex, 7.29µmol.L^{-1}.min^{-1} for the **L^4[Cu($CH_3COO)_2$]** and rate of 5.34µmol.L^{-1}.min^{-1} for **L^6[Cu($CH_3COO)_2$]** complex.

3.2.5. Effect of solvent

To understand better the effect of solvent on the catalysis of oxidation reaction of catechol, we carried out the same experiments under same thermodynamic conditions, but by using the

acetonitrile and THF as solvent, the absorbance of *o*-quinone are shown in Fig.6. The calculation of catechol oxidation rate in the presence of the copper complexes with ligands **L¹–L⁶** in the acetonitrile and THF, led to results gathered in Table 3. From results obtained by the spectrometer UV–vis and from reaction rates, we observed that the nature of used solvent has an important effect on the catalytic activities of the studied complexes. Methanol, protic and polar solvent, appears a better solvent than acetonitrile which is aprotic and polar solvent. If we consider that the commonly known physical parameters of solvents like dielectric constant, dipole moment, polarity, etc., have no significant role in changing the activity of the complexes toward the oxidation of catechol, it should be the coordination power or protic nature of the solvents that play the key role in changing the activity of the complexes [33].

3.3. Kinetic study

The reaction kinetics was studied by observing the time dependent change in absorbance at a wavelength of 390 nm for catalysis in MeOH with ligand **L¹**, concentration of **L¹** was fixed in 10^{-3}mol/L. 0.04 ml of the ligand solution, with a constant concentration of 1 M,was added to 2 ml of catechol of a particular concentration (concentration varying from 1.10^{-3} M to 1.10^{-2} M) to achieve the ultimate concentration of the ligand as 10^{-2}M. The conversion of catechol to *o*-quinone was monitored with time at a wavelength of 390 nm. The rate versus concentration of substrate data were analyzed on the basis of Michaelis–Menten approach of enzymatic kinetics to get the Lineweaver–Burk (double reciprocal) plot as well as the values of the various kinetic parameters (V_{max}=8.95 µmol.L^{-1} min^{-1} , K_M=0.0098 mol.L^{-1}).

The spectra of ligand **L¹** in methanol solution show dramatic changes immediately after addition of *o*-quinone. Fig.8 shows the variation of the spectral behaviour for **L¹** as representative of it followed up for 2 h. From the figure, it is clear that the bands at 268 and 355 nm vanishes immediately after addition of catechol, and three new bands are developed at 400, 500 and 680 nm. Also the d-d bands are retained even after 2 h of reaction, indicating the presence of Cu(II) species.

3.3.1. Catecholase mechanism

The mechanism for the enzymatic reaction is primarily based on an earlier proposal derived from spectroscopy and theoretical studies [34] and a recent series of crystal structures of the various intermediates of the catechol oxidase [35]. Two catechol molecules are oxidized per cycle and dioxygen is reduced to water.

In the first stage of the reaction, the dicopper (II) complex **1** reacts with dioxygen to form the *oxy* form (Cu^{II}–O_2^{2-}–Cu^{II}) species **2**. This species oxidizes one equivalent of catechol in stoichiometric reaction through a two-electron transfer from the catechol to the peroxide moiety. After the quinone molecule is released, the complex **4** (Cu^{II}-OH-Cu^{II}, met) is generated, and the catalytic cycle can continue, as shown in Scheme 3. Two equivalents of quinone are thus generated per one catalytic cycle. This mechanism is in fact very similar to the mechanisms earlier proposed by Wagner and *coll.* [36] and Rolff and *coll.*[37] for dinuclear Cu(II) complexes, and by Krebs and co-workers for catechol oxidase [38,39]. Although the binding mode of the substrate to the dicopper centers unfortunately remains unclear.

3.3.2. UV–vis spectrophotometric study for catechol oxidase activity of the complex

The catecholase activity of complex **CP_1** was studied in methanol–DMF (50:1, v/v). Fig.9 shows the change of spectral behavior of complex immediately after the addition of a solution of catechol to the complex solutions the original bands vanish.

In MeOH, *o*-quinone shows maximum absorption at 390 nm (Fig.9). *o*-quinone obtained was purified by column chromatography with yields 65.5%. This was characterized by determining its melting point (75-80°C) which agreed well with that reported in literature [40].

3.4. Oxidation of phenol: tyrosinase activities

The oxidation of phenol was realized by adding successively 0.334 mL of the ligand **L^1** (2×10^{-3} M) and 0.668 mL of metallic salt $Cu(CH_3COO)_2$ (2×10^{-3} M) in 2 mL of phenol (10^{-1} M), the spectrum of evolution of orthoquinone absorbance was registered according to time every 20 min**.** We have found that all ligand **L^1 –L^6** have no tyrosinase activity.

3.4. Theoretical calculations

To investigate the structure geometries, we performed full geometry optimization of **CP_1** and **CP_2** in the gas phase using DFT/B3LYP (C, H, N and O)/LanL2DZ (Cu) level calculations. Additionally to the geometry optimization, density functional theory has been found to be successful in providing insights into the chemical reactivity and stability, the analysis of the frontier molecular orbitals is a crucial way to obtain information on reactivity of molecules and to study electron excitation from the highest occupied molecular orbital (HOMO) to the lowest unoccupied molecular orbital (LUMO). The LUMO represents the ability of the molecule to capture an electron while the HOMO represents the ability to donate an electron.

The optimized structure (Fig.10) of **CP_1** display a coordination site of seven atoms that is formed by the two pyrazolic rings, the distance between sp^2 Nitrogen and Copper (N-Cu) are 1.96 Å, the two bonds (N-Cu) constitutes an angle of 102.65° (N-Cu-N) with Copper. For **CP_2** the coordinated coppers are in small cavities (five atoms) formed by sp^2 Nitrogen of pyrazole and quinoxalin rings. The angles N-Cu-N were equal to 82.43° and the bond length N-Cu varies from1.93 Å to 1.99 Å.

In **CP_1**, the occupied orbitals are mainly localized on the acetate fragment and the copper, while the unoccupied orbitals have their major contribution from the ligand. These results suggest that the transition involve charge transfer from the metal to ligand (MLCT). From MOs of **CP_2** it seems that there is a metal-metal charge transfer (MMCT) (Fig.11).

By using HOMO and LUMO energy values for a molecule, the global chemical reactivity descriptors of molecules such as hardness (η), softness (S),) can be measured by using Koopman's theorem for closed-shell molecules.

A molecule having high ionization potential (I) or electron affinity (A) loses or admits electron hardly [41,42]. By Koopmans' approximation [43.44], the ionization potential and electron affinity of any molecule can be calculated using the relations,

$I = -E_{HOMO}$ (1)

$A = -E_{LUMO}$ (2)

Koopmans` theorem for closed-shell molecules [44] results in the hardness of the molecule;

$\eta = (I-A)/2$ (3)

The softness of the molecule;

$S = 1/2\eta$ (4)

The hardness of a molecule is a qualitative indication of how polarizable it is, that is how much its electron cloud is distorted in an electric field. In this sense the terms hard, and its opposite soft, were evidently suggested by D.H. Busch [45] by analogy with the conventional use of these words to denote resistance to deformation by mechanical force. Absolute hardness, η, and softness, σ, are important properties to measure the molecular stability and reactivity. A hard molecule has a large energy gap and a soft molecule has a small energy gap. Soft molecules are more reactive than hard ones because they could easily offer electrons to an acceptor.

Using the above relations we find the electro molecular characteristics for **CP1** and **CP2** has been presented in Table 4.

Table 4 shows that **CP2** has lower energy gap (0.404 a.u). Lower hardness (0.202a.u), the higher softness (2.4752 a.u). The **CP1** has the higher energy gap (2.514a.u), higher hardness (1.257a.u), and a lower softness (0.3977a.u). A small energy gap are generally associated with a high chemical reactivity, low kinetic stability and are also considered as soft entities, while those with large energy gap have higher stability and are termed as hard molecules because they oppose charge transfer and changes in their electron density and distribution. The results indicate that compound $\mathbf{CP_2}$, with smaller LUMO/HOMO gap, is softer, less stable and more reactive than $\mathbf{CP_1}$.The ionization potential (I) of **CP1** and **CP2** molecules are 5.703a.u and 5.863a.u respectively. The electron affinity (A) for both molecules is 3.189 a.u and 5.459a.u for **CP1** and **CP2**, respectively, which clearly indicates that the $\mathbf{CP_1}$ are very stable than $\mathbf{CP_2}$.

4. Conclusion

Six ligands and a new complex were synthesized, which show efficacity in the oxidation rate of catechol in aerobic conditions. According to the obtained result ligand $\mathbf{L^1}$ exhibits a high rate of oxidation reaching to 33.48 $\mu mol.L^{-1}.min^{-1}$. At the same time, weak bonds of anions-metals favorite the reaction of oxidation as in the case of copper acetate. The presence of an electron-withdrawing group enrich the coordination properties of the ligands and gives stability to the complex, whereas the presence of donor group is a disadvantage for complex formation by decreasing the electron density on the sites of coordination (such as in $\mathbf{L^3}$). The study of various metals salts shows that the catalytic activities are most controlled by the nature of metal too. From the theoretical calculations, $\mathbf{CP_1}$ is more stable than $\mathbf{CP_2}$ and the charge transfer is from metal to ligand ($\mathbf{CP_1}$) and metal-metal charge transfer for $\mathbf{CP_2}$ (MMCT).

References

[1] R.Than, A.A. Feldmann, B. Krebs, *Coord. Chem. Rev.* 182, 211–241(1999).

[2] M.J. Alcon, M. Iglesias, F. Sanchez, *Inorg. Chim. Acta*, 333, 83-92(2002).

[3] W.A. Alves, S.A. de Almeida-Filho, M.V.de Almeida, A. Paduan -Filho, C.C. Becerra, A.M. Da Costa Ferreira, *J.Mol.Cat.Chem.*, 198, 63–75(2003).

[4] M.E. Cuff, K.I. Miller, K.E. Van Holde, W.A. Hendrickson, *J. Mol. Biol.*, 278, 855–870(1998).

[5] R.D. Swerdlow, R.F. Ebert, P. Lee, C. Bonaventura, K.I. Miller, *Comp. Biochem. Physiol.*, 537-548(1996).

[6] V. Amore, B. Gaetani, M.A. Puig, R. Fochetti, *J. Ins. Sci.*, 11, 153-158(2011).

[7] M. Tareq, H. Khan, *Pure Appl. Chem.,* 79, 2277–2295(2007).

[8] J.P. Germanas, S. Wang, A.Miner,W. Haob, J.M. Ready, *Bioorg. Med. Chem. Letters*, 17, 6871–6875(2007).

[9] N. Boussaleh, R. Touzani, I. Bouabdallah, S. Ghalem, S. El Kadiri, *Int. J. Acad. Res*., 2,137–143(2009).

[10] A. Zerrouki, R. Touzani, S. El Kadiri, *Arab. J. Chem.* 4, 459–464(2011).

[11] S. Thabti, A. Djedouani, S. Rahmouni, R. Touzani, A. Bendaas, H. Mousser, *J. Mol. Struc.,* 1102, 295-301(2015).

[12] I. Bouabdallah, R. Touzani, I. Zidane, A. Ramdani, *Catal. Commun*., 8, 707–712(2007).

[13] A. Mouadili, A. Attayibat, S. El Kadiri, S. Radi, R. Touzani, *Applied Catalysis A General*, 454, 93-99(2013).

[14] A. Djedouani, F. Abrigach, M. Khoutoul, A.Mohamadou, A. Bendaas, A.Oussaid, R.Touzani. *Oriental Journal of Chemistry 3*1(1), 97-105(2015).

[15] A. Mouadili, A. El Ouafi, A. Attayibat, S. Radi, R. Touzani, *J. Mater. Environ. Sci.,* 6, 2166-2173(2015).

[16] L. Michaelis, M.L. Menten, *Biochem.* Z. 49,333–369(1913).

[17] H. Narayan Mishra, *J. Mol. Str.*, 1022, 49-60(2012).

[18] P.E.M. Siegbahn, T. Borowski, *Acc. Chem. Res*. 39, 729(2006).

[19] P.E.M. Siegbahn, *J. Biol. Inorg. Chem.* 11, 695(2006).

[20] M.R.A. Blomberg, P.E.M. Siegbahn, J. Comput. Chem. 27, 1373(2006).

[21] A. Bassan, M.R.A. Blomberg, T. Borowski, P.E.M. Siegbahn, *J. Inorg. Biochem*. 100, 727(2006).

[22] D. Sandhya Rani, P.V. Anantha Lakshmi, V. Kamala Prasad, V. Jayatyaga Raju, Chin. *J. Inorg. Chem.,* 28, 1245-1250(2012).

[23] Z. Bouanane, M. Bounekhel, M. Elkoli, A. Takfaoui, F. Abrigach, R. Boyaala, R.Touzani, Maghr. *J. Pure Appl. Sci.*1, 62-73(2015).

[24] M.J. Frisch, G. W. Trucks, H. B. Schlegel, G. E. Scuseria, M. A. Robb, J. R. Cheeseman, G. Scalmani, V. Barone, B. Mennucci, G.A. Petersson, H. Nakatsuji, M. Caricato, X. Li, H. P. Hratchian, A.F. Izmaylov, J. Bloino, G. Zheng, J.L. Sonnenberg, M. Hada, M. Ehara, K. Toyota, R. Fukuda, J. Hasegawa, M. Ishida, T. Nakajima, Y. Honda, O. Kitao, H. Nakai, T. Vreven, J. A. Montgomery, Jr., J. E. Peralta, F. Ogliaro, M. Bearpark, J. J. Heyd, E. Brothers, K. N. Kudin, V. N. Staroverov, R. Kobayashi, J. Normand, K. Raghavachari, A. Rendell, J.C. Burant, S. S. Iyengar, J. Tomasi, M. Cossi, N. Rega, J. M. Millam, M. Klene, J. E. Knox, J.B. Cross, V. Bakken, C. Adamo, J. Jaramillo, R. Gomperts, R. E. Stratmann, O. Yazyev, A.J. Austin, R. Cammi, C. Pomelli, J.W. Ochterski, R.L. Martin, K. Morokuma, V.G. Zakrzewski, G.A. Voth, P. Salvador, J.J. Dannenberg, S. Dapprich, A. D. Daniels, O. Farkas, J.B.

Foresman, J.V. Ortiz, J. Cioslowski, and D.J. Fox, Gaussian 09, Revision A.02, Gaussian, Inc., Wallingford CT,(2009).

[25] GaussView, Version 5, Roy Dennington, Todd Keith, and John Millam, Semichem Inc., Shawnee Mission, KS, (2009).

[26] A.D. Becke, *J. Chem. Phys.* 98, 5648-5652(1993).

[27] C. Lee, W. Yang, R.G. Parr, *Phys. Rev. B* 37, 785-789(1988).

[28] P.J. Hay, W.R. Wadt, *J. Chem. Phys.* 82, 270-299(1985).

[29] C.A. Obafemi, W. Pfleiderer, *Helv. Chim.Acta.* 77, 1549 – 1556(1994).

[30] M.M. Badran, K. A. M. Abouzid, M. H. M. Hussein, *Transition Metal Chemistry*, 19, 75-77(1994).

[31] A. Takfaoui, M. Lamsayah, A. El Ouafi, A. Oussaid, Z. Kabouche, R. Touzani; *J. Mater. Environ. Sci.* 6, 2129-2136(2015).

[32] R.N Mukherjee, *Ind. J. Of Chem.*, 42A, 2175-2184 (2003).

[33] K.S. Banu, M. Mukherjee, A. Guha, S. Bhattacharya, E. Zangrando, D. Das, *Polyhedron* 45, 245–254(2012).

[34] E.I. Solomon, U. M. Sundaram, T. E. Machonkin, *Chem. Rev.* 96, 2563-2605(1996).

[35] T. Klabunde, C. Eicken, J. C. Saccettini, B. Krebs, *Nat. Struct. Biol.* 5, 1084-1090(1998).

[36] R.Wegner, M. Gottschaldt, H. Görls, E.G. Jäger, D. Klemm, *Chem. Eur. J.*, 7, 2143-2157(2001).

[37] A. Hoffmann, C. Citek, S. Binder, A. Goos, M. Rübhausen, O. Troeppner, I. I.Burmazović, E.C. Wasinger, T.D.P. Stack, S. Herres-Pawlis. *Angew. Chem. Int. Ed. Engl.*, 52, 1-10(2013).

[38] C. Eicken, B. Krebs, J.C. Sacchettini, *Curr. Opin.Struct. Biol.* 9, 677-683(1999).

[39] Z. Qian, H. Yan, J. Yuan-Hong, Synthesis, *Chin. J. Inorg. Chem.*, 32, 131-138(2016).

[40] K.T. Finley,; Polyhedron,*Ullmann's Encyclopedia of Industrial Chemistry*, *Benzoquinone*. Wiley-VCH Verlag GmbH & Co, 343-347(2002).

[41] K. Govindarasu, E. Kavitha *Spectrochimica Acta Part A*, 133: 799-810(2014).

[42] D.M. Burland, R.D. Miller, C.A.Walsh, *Chem. Rev*. 94: 31-75(1994).

[43] V.M. Geskin, C. Lambert, J.L. Brédas, *J. Am. Chem. Soc*. 125: 15651-15658(2003).

[44] D.A. Kleinman, *Phys. Rev.* 126: 1962-1979(1977).

[45] R. G. Pearson, *J. Am. Chem. Soc*., 85, 3533(1963). (b) R. G. Pearson, Science, 1963,151, 172 (1963).

Figures and Schemes captions

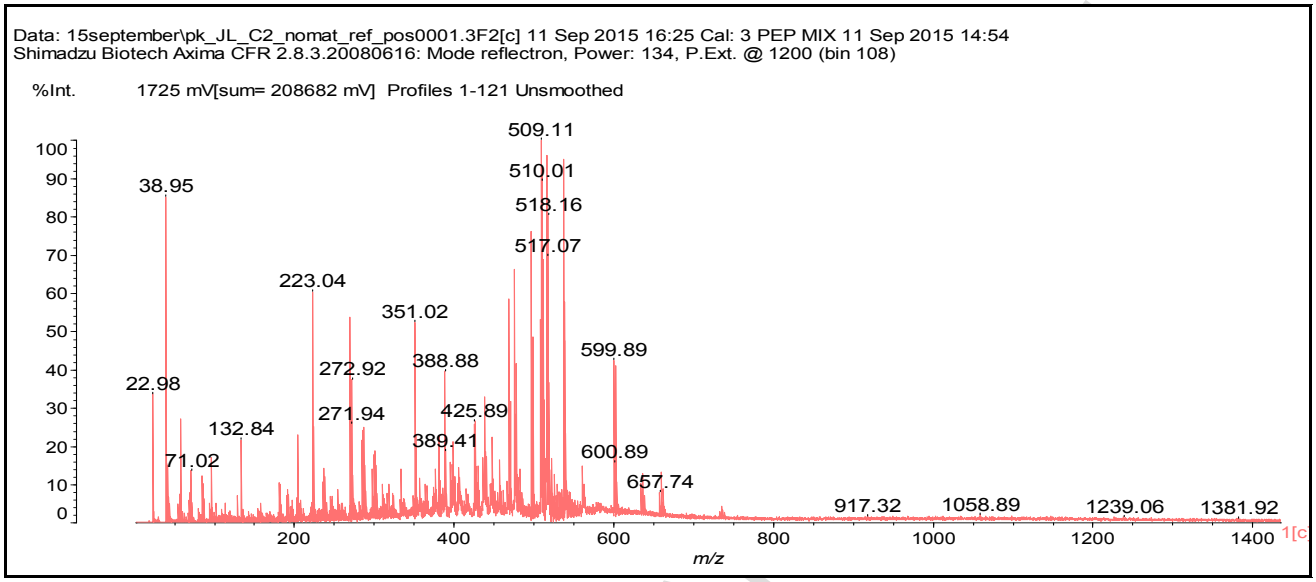

Fig.1. MALDI-TOF mass spectrum of **CP_1.**

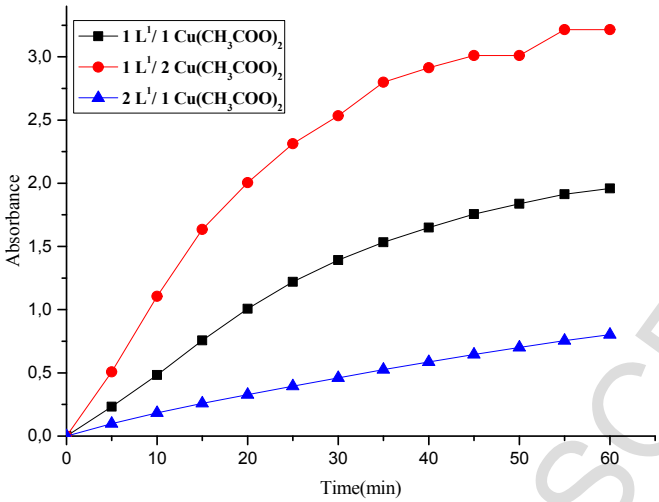

Fig.2. Oxidation of catechol by complexes of ligand $\mathbf{L^1}$.

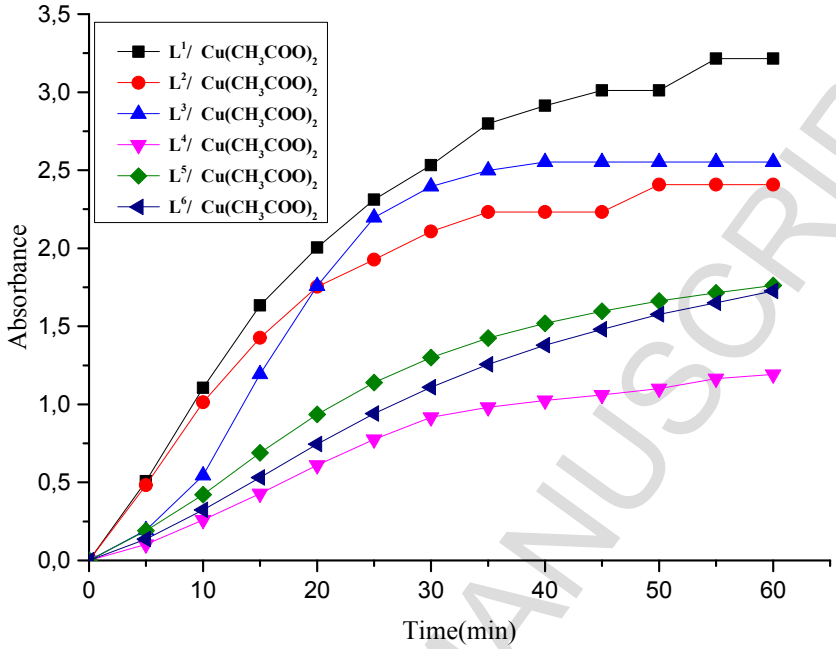

Fig.3. Oxidation of catechol by complexes of ligand **L^1-L^6 (**1 equiv **L** / 2 equiv **M).**

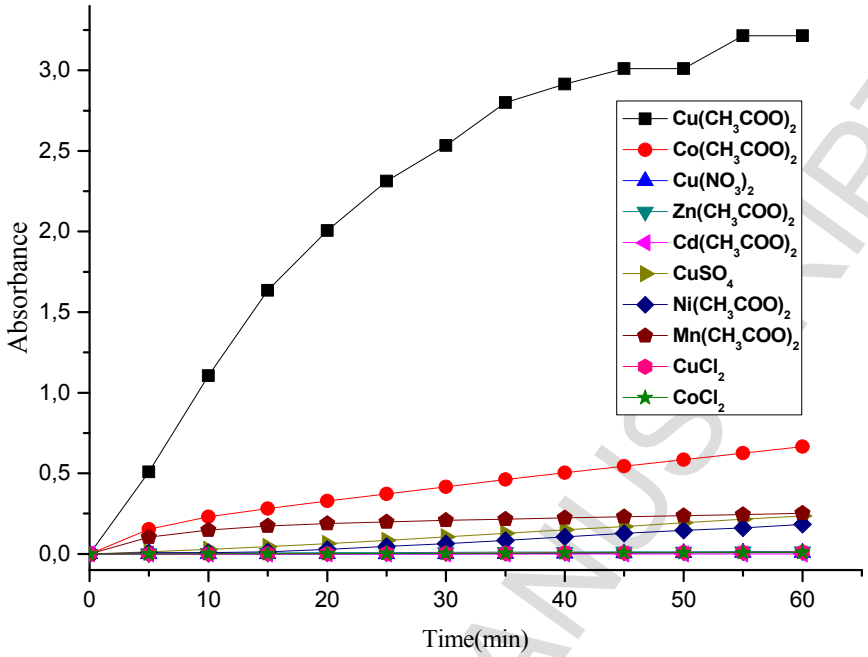

Fig.4. Oxidation of catechol by complexes of ligand **L^1 (1 equiv L /2 equiv M).**

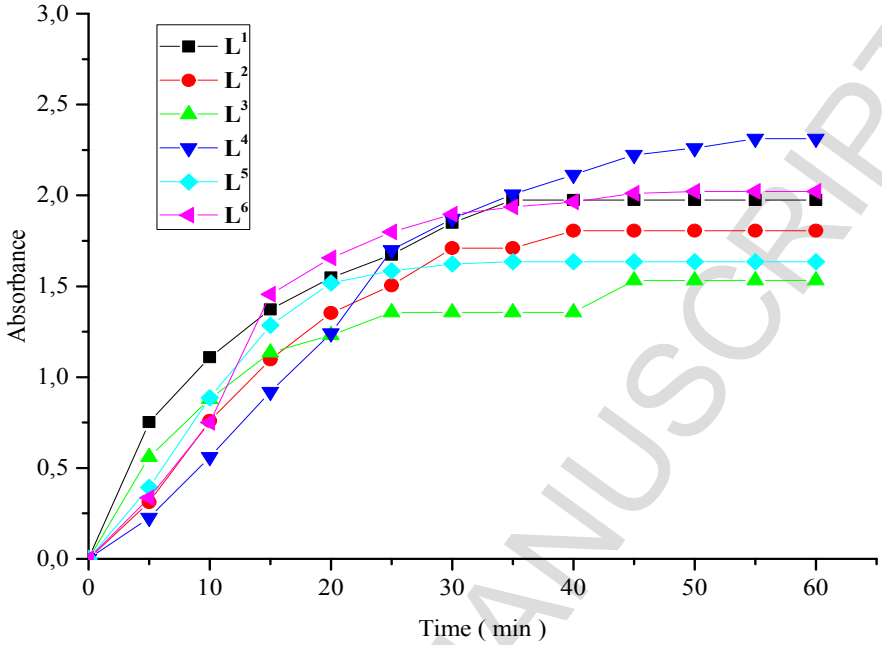

Fig.5. 3,5-DTBQ oxidation in presence of ligand **L^1-L^6** (1equiv **L**/2 equiv **$Cu(CH_3COO)_2$**).

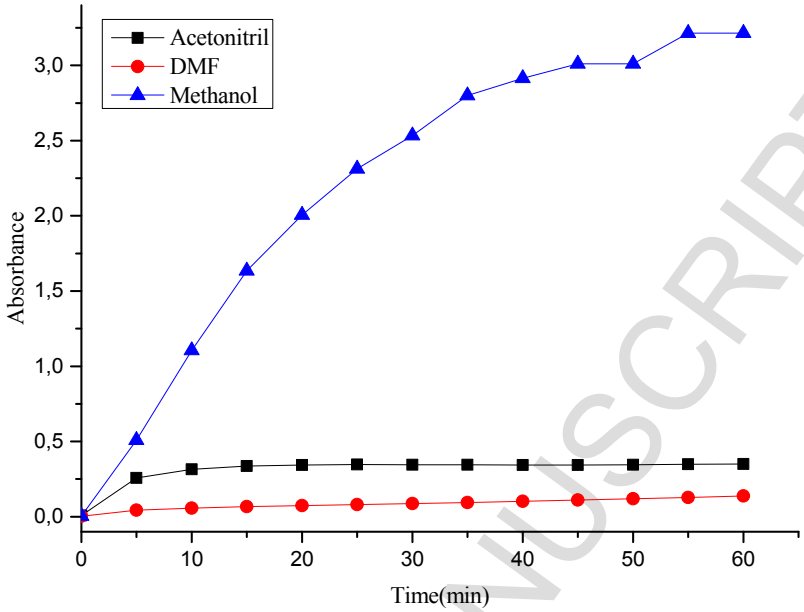

Fig.6. Catechol oxidation in presence of **L^1/ $Cu(CH_3COO)_2$ (1 equiv L /2 equiv M)** in different solvents.

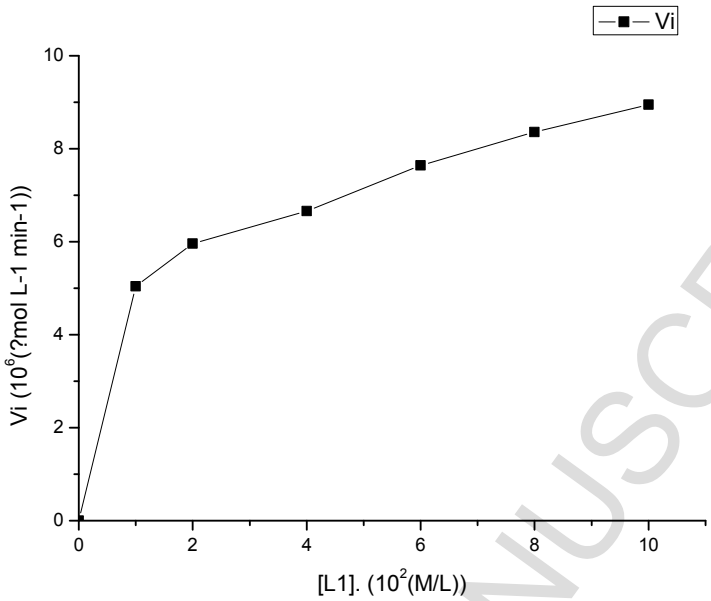

Fig.7. Dependence of the reaction rates on the catechol concentrations for the oxidation reaction from one equivalent of **L^1** and two equivalents of **$Cu(CH_3COO)_2$** (in methanol).

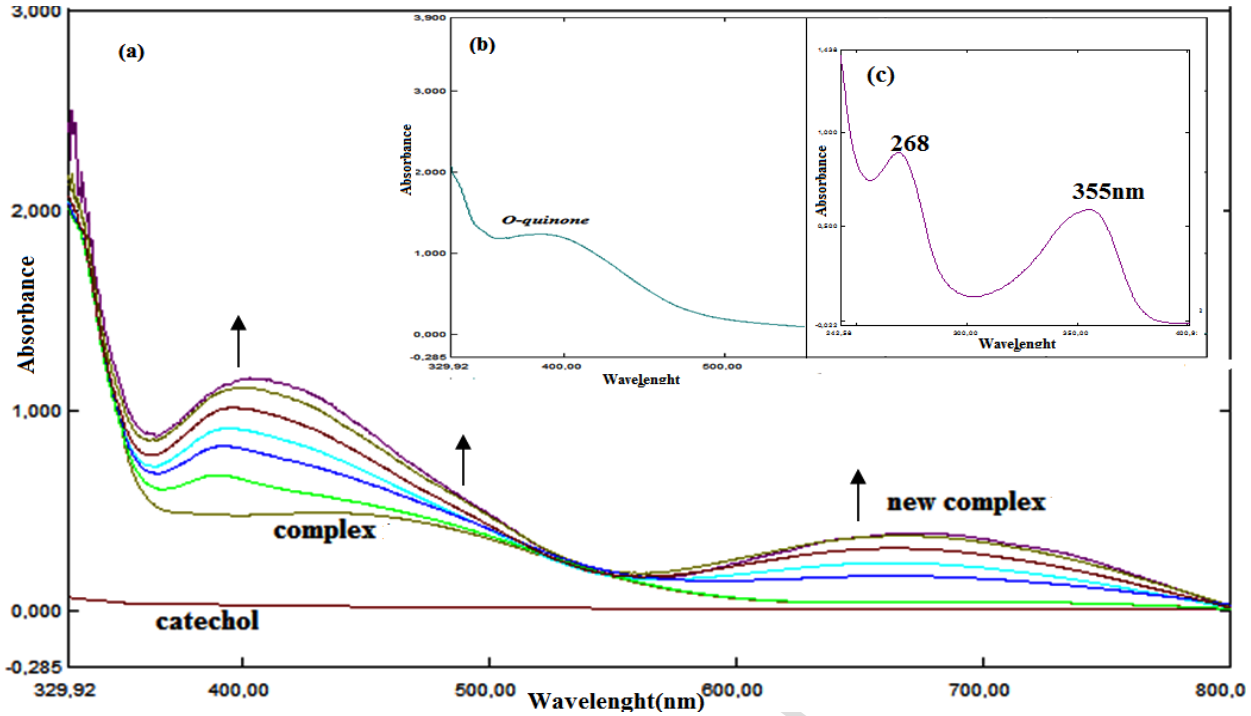

Fig.8. (a) The variation of the spectral behavior after addition of catechol (1:100) to methanol solution of ligand $\mathbf{L^1}$ followed up for 2 h. The spectra are recorded every 20 min. (b) final spectrum of solution after 24 h. (c) spectrum of ligand $\mathbf{L^1}$ in methanol.

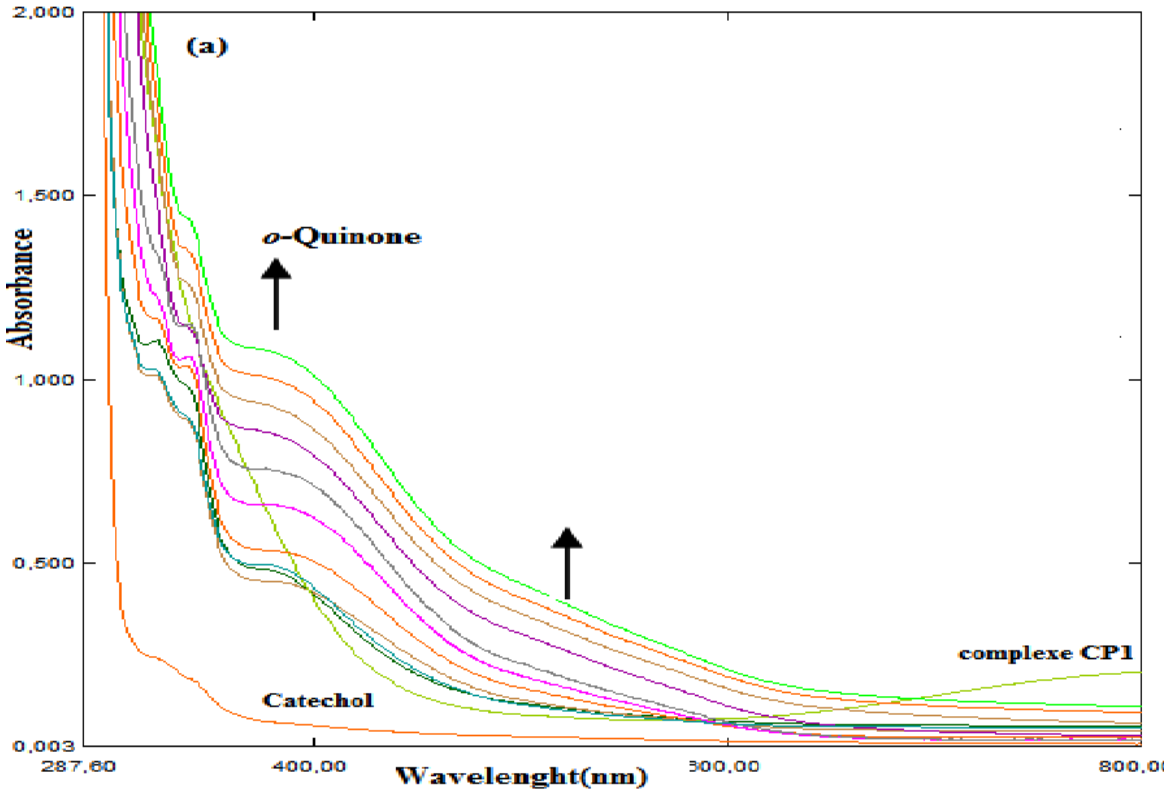

Fig.9. (a) Variation of the spectral behaviour after addition of catechol (1:100) to methanol-DMF (50/1, v/v) solution of complex $\mathbf{CP_1}$ followed up for 2 h. The spectra are recorded every 20 min.

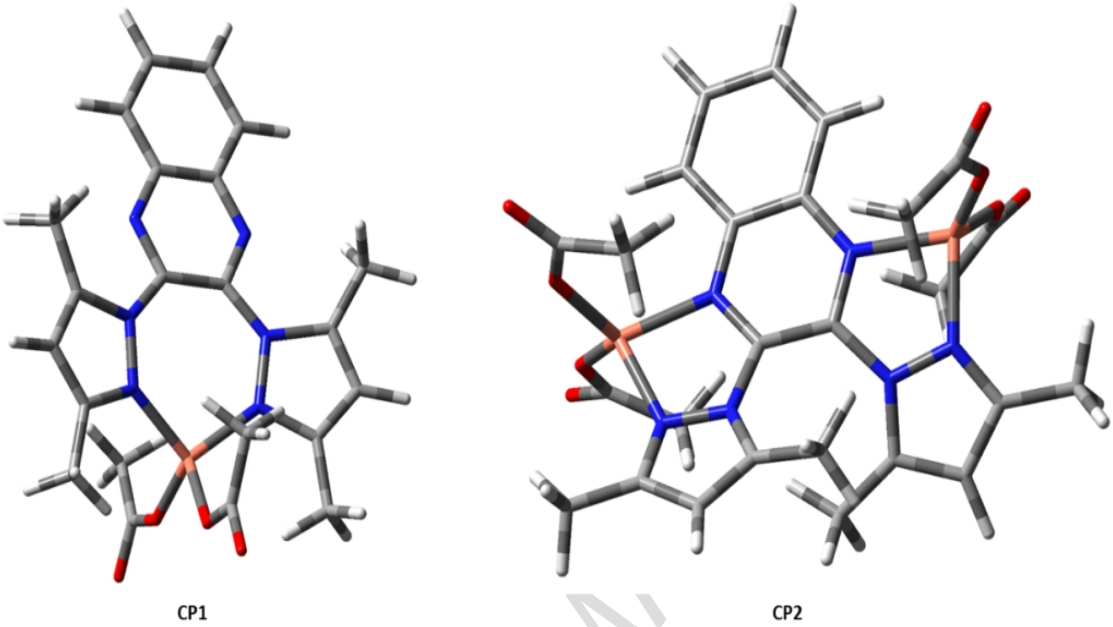

Fig.10. Optimized geometries of $\mathbf{CP_1}$ and $\mathbf{CP_2}$.

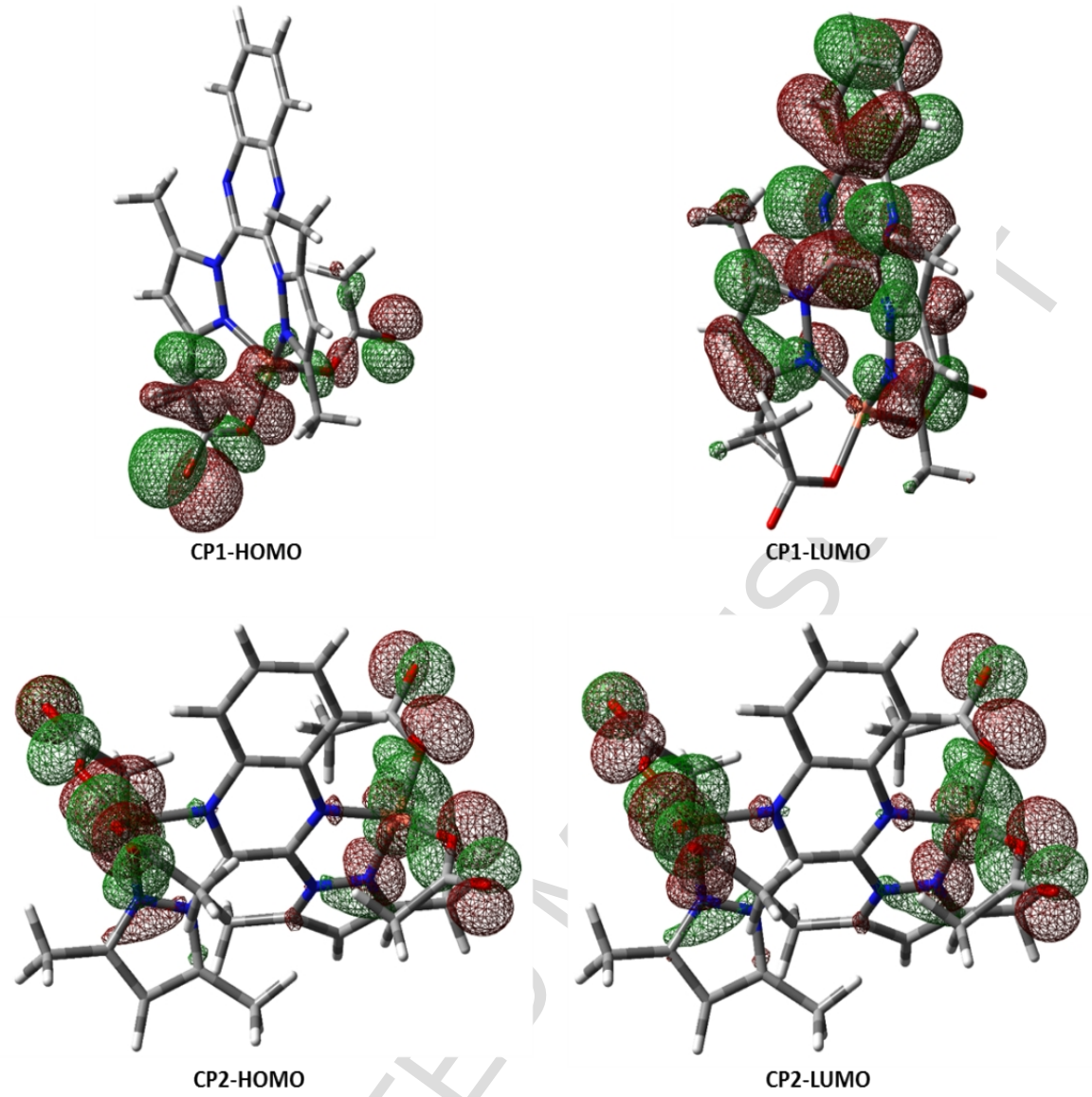

Fig.11. Orbitals frontiers of $\mathbf{CP_1}$ and $\mathbf{CP_2}$.

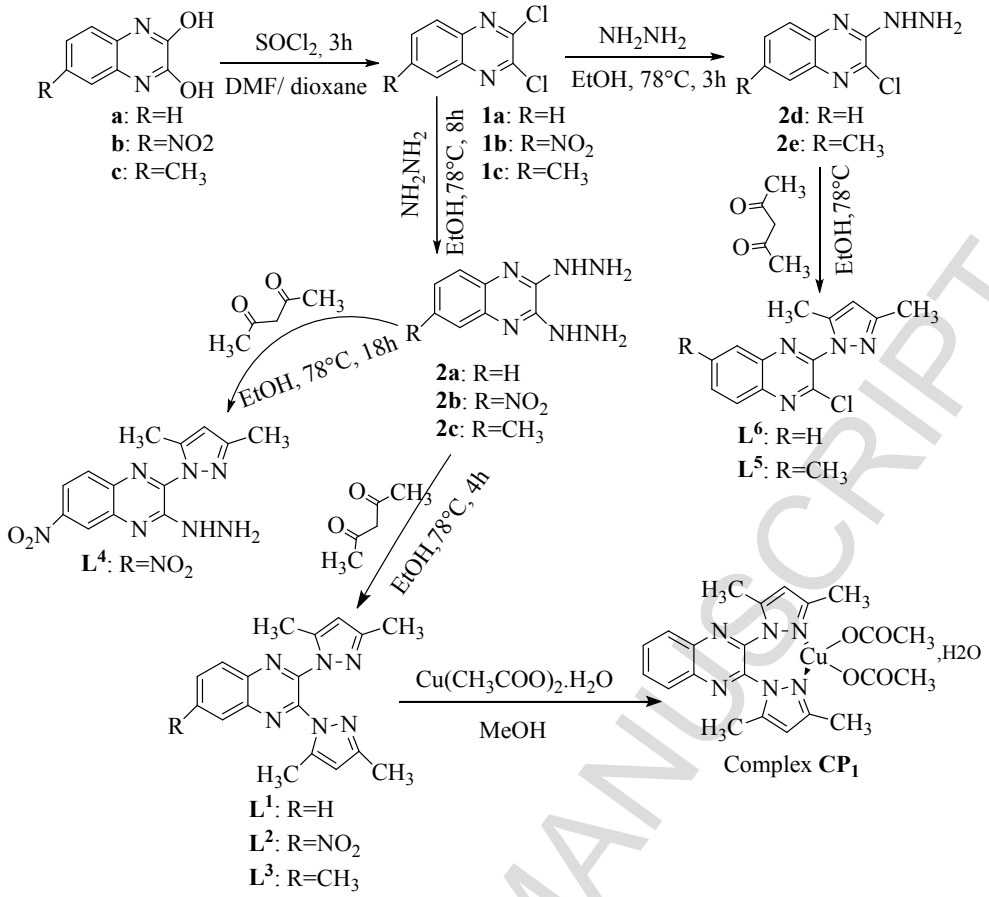

Scheme 1. Reaction pathway for $\mathbf{L^1}$, $\mathbf{L^2}$, $\mathbf{L^3}$, $\mathbf{L^4}$, $\mathbf{L^5}$ and $\mathbf{L^6}$.

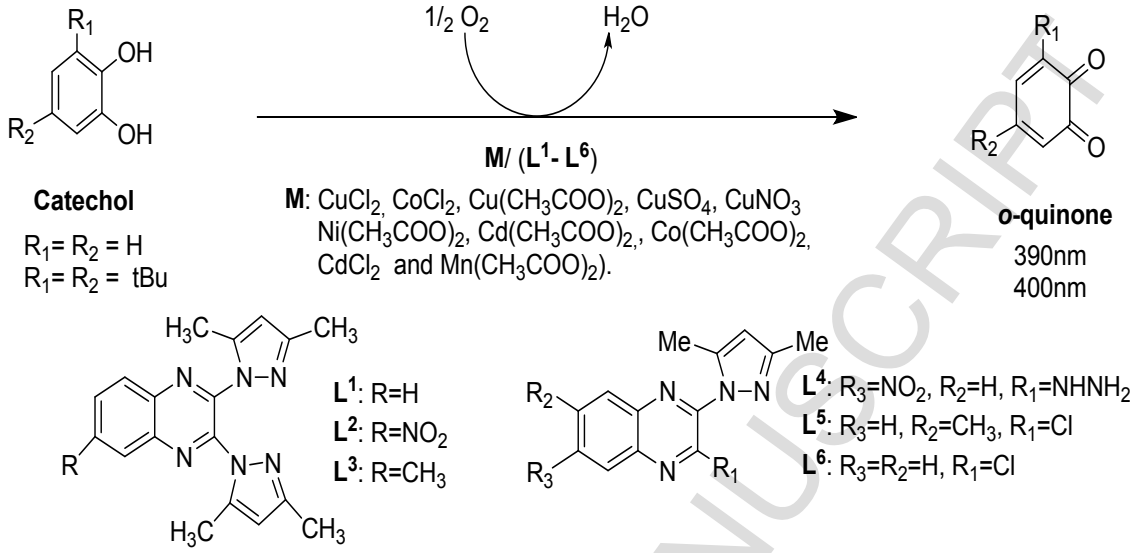

Scheme 2. Oxidation of catechol to *o*-quinone.

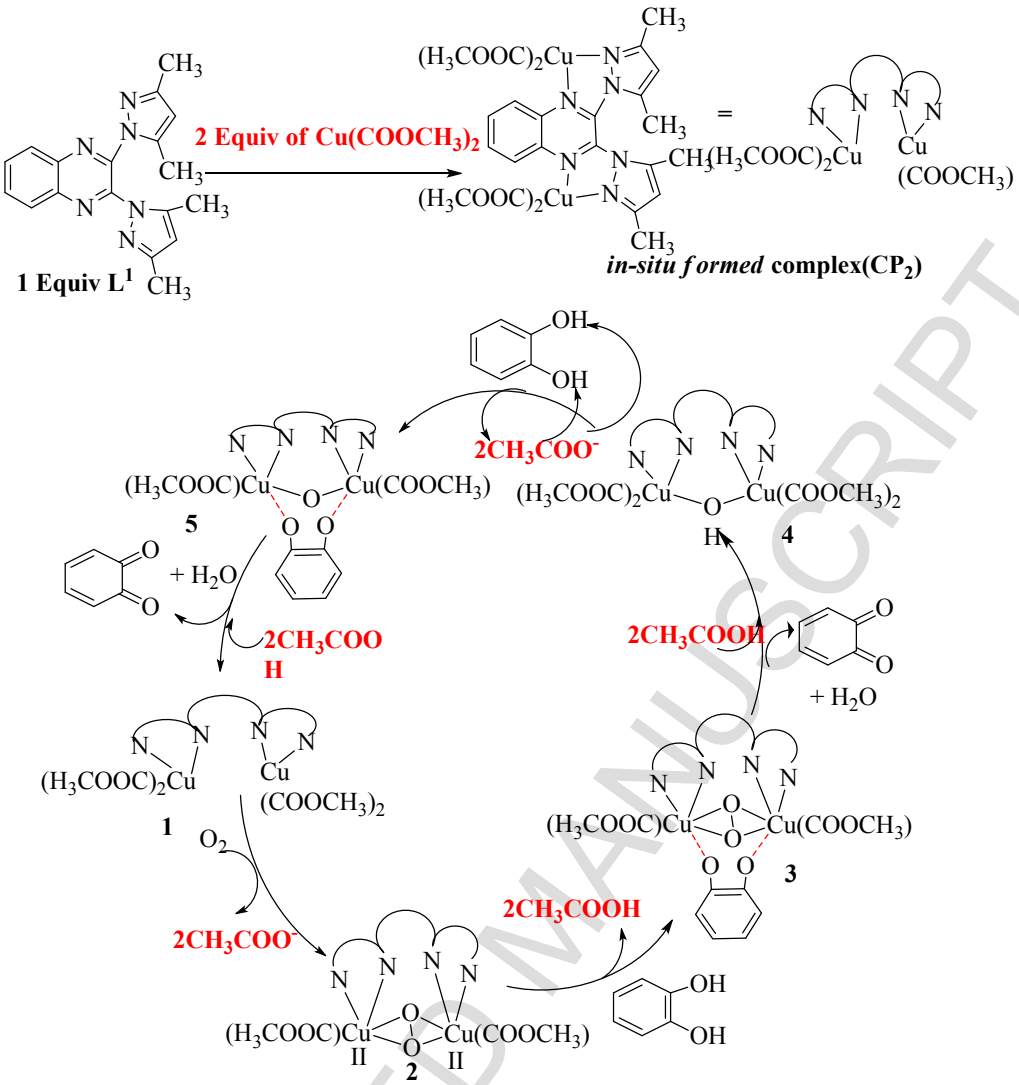

Scheme 3. Proposed mechanism for the catechol oxidation using **L^1/ $Cu(CH_3COO)_2$** system.

Table captions

Table 1.

Oxidation rates (μmol.L^{-1}.min^{-1}) of catechol in presence of Ligand **L^1-L^6** with $Cu(CH_3OO)_2$ in MeOH.

Ligand / metallic salt	1equiv / 1 equiv	1 equiv / 2 equiv	2 equiv/ 1 equiv
L^1	20.04	**33.48**	8.36
L^2	25.08	**31.95**	15.83
L^3	23.15	**26.58**	18,31
L^4	18.35	**24.08**	10.79
L^5	17.98	**20.16**	12.75
L^6	12.41	**17.02**	18.07

Table 2.

Oxidation rates (μmol. L^{-1}. min^{-1}) of catechol.

L/M	$Cu(OAc)_2$	$Cu(NO_3)_2$	$CuSO_4$	$Co(OAc)_2$	$Mn(OAc)_2$	$Cd(OAc)_2$	$Ni(OAc)_2$	$CoCl_2$	$CuCl_2$
L^1	**33.48**	0.09	2.45	6.92	2.62	0.04	1.90	1.02	1.10
L^2	**31.95**	0.06	6.08	5.92	1.92	0.36	1.49	0.06	0.11
L^3	**26.58**	0.50	2.14	6.89	2.38	0.03	1.61	0.30	0.06
L^4	**24.08**	0.68	2.22	7.10	2.29	0.03	1.66	0.04	0.10
L^5	**20.16**	0.29	0.53	8.42	3.18	0.13	2.23	0.04	0.17
L^6	**17.02**	0.08	2.21	6.97	2.39	0.03	1.83	0.06	0.04

Table 3.

Oxidation rates (μmol.L^{-1}.min^{-1}) of catechol in presence of Ligand **L^1-L^6** with $Cu(CH_3COO)_2$ **(1** equiv **L** /**2** equiv **M)** in different solvents.

Ligand / metallic salt	DMF	methanol	Acetonitrile
L^1	1.38	**33.48**	3.65
L^2	1.04	**31.95**	1.53
L^3	0.36	**26.58**	0.94
L^4	-	**18.53**	-
L^5	-	**17.98**	-
L^6	-	**17.02**	-

Table 4.

Calculated energies of **CP_1** and **CP_2.**

Molecular Energy(a.u)	**CP_1**	**CP_2**
E(B3LYP)	-45667.352	-63440.044
E_{LUMO}	-3.189	-5.459
E_{HOMO}	-5.703	-5.863
Energy gap (Δ)	2.514	0.404
Ionization Potential (I)	5.703	5.863
Electron affinity (A)	3.189	5.459
Global Hardness (η)	1.257	0.202
Global Softness (*s*)	0.3977	2.4752